

Review

# Toxicity Analysis of Nano-Minimum Quantity Lubrication Machining—A Review

Ibrahim Nouzil <sup>1</sup>, Abdelkrem Eltaggaz <sup>1,\*</sup> , Salman Pervaiz <sup>2</sup>  and Ibrahim Deiab <sup>1</sup> <sup>1</sup> School of Engineering, University of Guelph, Guelph, ON N1G 2W1, Canada<sup>2</sup> Department of Mechanical Engineering, Rochester Institute of Technology, Dubai P.O. Box 341055, United Arab Emirates

\* Correspondence: aeltagga@uoguelph.ca

**Abstract:** The lubrication properties of nanoparticles are of great interest to the manufacturing industry and led to the development of the nano-minimum quantity lubrication (NMQL) cooling strategy. To evaluate the sustainability characteristics of nano-minimum quantity lubrication, apart from analyzing the benefits of increasing machining efficiency, it is also essential to evaluate the potential detrimental effects of nanoparticles on human health and the environment. Existing literature provides substantial data on the benefits of nano-minimum quantity lubrication machining. However, the current literature does not provide researchers in the machining sector a comprehensive analysis of the toxicity of the nanoparticles used in nano-minimum quantity lubrication. This study aims to provide a comprehensive review that addresses the toxicity levels of the most frequently used nanoparticles in NMQL machining. To understand the impacts of nanoparticles on the human body and the environment, in vitro studies that evaluate the nanoparticles' toxicity on human cells and in vitro/in vivo studies on other living organisms are considered. The results from toxicity studies on each of the chosen nanoparticles are summarized and presented in chronological order. The reviewed studies indicate transition metal dichalcogenides (MoS<sub>2</sub> and WS<sub>2</sub>) exhibit very low toxicity when compared to other nanoparticles. The toxicity of hBN and AL<sub>2</sub>O<sub>3</sub> nanoparticles varies depending on their lengths and crystalline structures, respectively. In conclusion, a chart that maps the toxicity levels of nanoparticles on seven different human cell lines (human lung epithelial cells (A549), human bronchial epithelial cells (NI-20), AGS human gastric cells, human epidermal cells (HEK), human liver-derived cells (HepG2), human endothelial cells and human peripheral cells), representing exposures by inhalation, ingestion and dermal contact, was developed for easy and quick insights. This is the first attempt in open literature to combine the results of the experimental investigations of nano-minimum quantity lubrication cooling and the toxicity studies of nanoparticles, allowing researchers to make informed decisions in the selection of the most sustainable nanoparticles in the nano-minimum quantity lubrication machining process.

**Keywords:** toxicity; nano-MQL; machining; sustainability; minimum quantity lubrication

**Citation:** Nouzil, I.; Eltaggaz, A.; Pervaiz, S.; Deiab, I. Toxicity Analysis of Nano-Minimum Quantity Lubrication Machining—A Review. *Lubricants* **2022**, *10*, 176. <https://doi.org/10.3390/lubricants10080176>

Received: 10 June 2022

Accepted: 3 August 2022

Published: 6 August 2022

**Publisher's Note:** MDPI stays neutral with regard to jurisdictional claims in published maps and institutional affiliations.



**Copyright:** © 2022 by the authors. Licensee MDPI, Basel, Switzerland. This article is an open access article distributed under the terms and conditions of the Creative Commons Attribution (CC BY) license (<https://creativecommons.org/licenses/by/4.0/>).

## 1. Introduction

The machining and manufacturing sectors are among the most influential markets today with over 100 billion dollars in annual expenditures in the United States alone [1]. The importance of sustainability in machining processes is shown by the sheer volume of production involved and the corresponding potential environmental hazards. The dry machining of metals involves a very high generation of heat in the cutting zone and high cutting forces, which leads to tool wear, workpiece hardening and an increased surface roughness. To minimize these effects, lubrication and cooling via flood cooling techniques are generally employed in machining processes; however, the storage, use and disposal of these conventional lubricants have resulted in an increased environmental impact. Furthermore, due to their inherent toxicity, some lubricants are harmful to machine

operators. To avoid the excessive use of cutting fluids, and thereby reduce the potential environmental hazards, many researchers have studied minimum quantity lubrication (MQL) as a viable alternative [2], and literature provides positive results for MQL [3–5]. The MQL technique works with a flow rate of about 50 mL/h to 2000 mL/h, while the conventional flood cooling flow rate is approximately  $1200 \times 10^3$  mL/h [6,7]. However, the benefits of the MQL technique are limited due to the low cooling capacities of base fluids and the clogging of debris at the cutting zone when MQL is applied [8,9]. Nano-minimum quantity lubrication (NMQL) was developed to overcome the shortcomings of regular MQL.

Nanoparticles added to a base oil enhance the thermal conductivity of the resultant nanofluid. Therefore, machining with the NMQL technique reduces the cutting tool temperature due to an increased heat transfer coefficient. Further, a nanoparticle rolling effect at the cutting edge reduces contact friction and results in reduced contact forces [10,11]. Zhang et al. conducted studies to investigate the effectiveness of the NMQL grinding of grade 45 steel with MoS<sub>2</sub> nanoparticles immersed in different vegetable oils [12]. The authors employed a 2% and a 5% MoS<sub>2</sub> mass fraction and used four different base oils: liquid paraffin, palm oil, rapeseed oil and a combination of palm oil and soybean oil. Palm oil with MoS<sub>2</sub> nanoparticles was observed to provide the best results. Increasing the mass fraction up to 6% produced an improved lubricating performance, while at a mass fraction exceeding 6%, a deteriorating lubrication effect was the result. Kumar et al. compared the effectiveness of different mono and hybrid nanofluids in the grinding process of silicon nitride [13] and reported positive results with NMQL. A cutting fluid with mono nanoparticles (NPs) performed subpar compared to a fluid with hybrid NPs. Among the mono NPs, MoS<sub>2</sub> resulted in a lower grinding force, surface finish and specific grinding energy while a MoS<sub>2</sub>-WS<sub>2</sub> hybrid performed the best overall. The authors further stated that with dry and flood cooling, the grinding forces started to increase over time; however, when a nanoparticle jet MQL (NJMQL) was employed, the grinding forces were constant. The lubrication capability was also increased with NPs, and this was supported by the formation of small, segmented chips when an NJMQL was employed. Similarly, Roshan et al. reported a superior performance with Al<sub>2</sub>O<sub>3</sub> nanoparticles mixed with palm oil in a NJMQL setup for grinding Inconel 718 [14]. The authors reported the lowest specific grinding energy for a 0.5% wt. of NPs and a lower surface roughness for a 1% wt. of NPs. The increase in the surface quality with an increase in the NPs was attributed to better lubrication. This was facilitated by a rolling effect of the NPs at the cutting interface and a superior cooling ability of the NPs due to their high thermal conductivity.

Eltaggaz et al. investigated the influence of NMQL in the turning of austempered ductile iron (ADI) [15]. An oxide of aluminum with an  $\alpha$  nanocrystalline structure was dispersed in the air–oil mixture. NMQL performed better than the pure MQL and reduced the flank wear. A comparative study conducted by the authors to evaluate the advantages of various cooling strategies (dry, flood, MQL and NMQL) found that NMQL machining performed better than the base MQL and was comparable to flood cooling [16]. The authors conducted further studies in the machining of titanium with Al<sub>2</sub>O<sub>3</sub> nanoparticles and found that the seizure zone was reduced by using NMQL when compared to the base MQL cooling [17]. Further, the authors concluded that nanoparticle concentration positively impacted the tool life and quality of the surface finish. Further improvements in milling performance were reported in studies on ferritic stainless steel [18] and TiAlN-coated carbide surfaces [19] using graphene and hBN nanoparticles. Table 1 provides a summary of the studies on nano-MQL cooling and highlights the important conclusions drawn by the authors.

**Table 1.** Machining processes and materials studied in the literature on NMQL cooling strategy.

Process	Workpiece	Nanoparticle Used	Conclusion	Reference
Grinding	45 steel	MoS <sub>2</sub>	NMQL provided a better surface finish than MQL and dry cooling. Ra and SGE provided almost the same as flood cooling.	[12]
	Silicon nitride	MoS <sub>2</sub> -WS <sub>2</sub> , WS <sub>2</sub> -hBN, MoS <sub>2</sub> -hBN, AL <sub>2</sub> O <sub>3</sub> , ZnO and B <sub>4</sub> C	NMQL performed best with lower SGE and cutting forces compared to wet and MQL cooling. MoS <sub>2</sub> performed best among the mono NPs. Among the hybrids, MoS <sub>2</sub> -WS <sub>2</sub> and MoS <sub>2</sub> -hBN provided the best lubrication.	[13]
	Inconel 718	AL <sub>2</sub> O <sub>3</sub>	NMQL provided a better Ra and lower energy compared to pure MQL.	[14]
Turning	Inconel	hBN and AL <sub>2</sub> O <sub>3</sub>	0.5% vol. hBN performed better than pure MQL and dry cooling. It yielded a low tool wear and roughness. 0.5% hBN + LN <sub>2</sub> provided the best results in terms of interface temperature and Ra.	[20,21]
	Nimonic 90	AL <sub>2</sub> O <sub>3</sub>	Cryogenic cooling was concluded to be superior to NMQL.	[22]
Milling	Inconel X750	hBN, MoS <sub>2</sub> and graphite	0.5% hBN was found to have superior performance.	[23]
	Ferritic stainless steel ASI 430	Graphene	NMQL performed better. It improved the initial flank wear.	[18]
	TiAlN-coated carbide surface	Graphite (xGnP) and hBN (XGS)	A reduction in the friction coefficient was observed due to an expanding processing envelope of MQL due to the nanoplatelets.	[19]

The increased performance of the NMQL cooling strategy can be attributed to two factors: an increased thermal conductivity of the base oil due to the addition of highly conductive nanoparticles, which resulted in an increased heat removal rate and reduced friction induced by the rolling effect of nanoparticles at the tool–chip interface. The increased nanoparticle concentration developed a thick protective layer on the tool and work surface [16]. The reduction in friction was achieved by reducing the contact between the tool and the workpiece. An exaggerated view of the tool–chip contact interface in an NMQL cooling process is shown in Figure 1. The nanoparticles in the base oil produce a rolling effect and thereby increase the sliding action of the tool, therefore reducing the friction. The highlighted studies clearly indicate a positive effect of using the NMQL cooling strategy. From Table 1 and an existing review paper [24] on NMQL machining, the most frequently used nanoparticles are tungsten disulfide (WS<sub>2</sub>), molybdenum disulfide (MoS<sub>2</sub>), boron nitride (BNNT and hBN), carbon nanotubes (CNT, SWCNT and MWCNT) and oxides of zinc (ZnO) and aluminum (AL<sub>2</sub>O<sub>3</sub>).

The science of sustainability addresses all the different aspects involved in the development and the use of any technology. To evaluate the sustainability characteristics of nano-minimum quantity lubrication, apart from analyzing the benefits of increasing machining efficiency, it is also essential to evaluate the potential detrimental effects of nanoparticles on human health and the environment. As was highlighted, the existing literature provides substantial data on the benefits of the NMQL machining process when compared to pure MQL and other conventional cooling strategies [3,25,26]. However, the current literature does not provide researchers in the machining sector a comprehensive analysis of the toxicity of the nanoparticles used in nano-minimum quantity lubrication. Pereira et al. conducted a lifecycle assessment to study the environmental effects of the biodegradable oils used in minimum quantity lubrication [27], but similar studies are lacking in the field of nano-MQL lubrication. The current study aims to provide a compre-

hensive review that addresses the toxicity levels of the most frequently used nanoparticles in NMQL machining. To understand the impacts of nanoparticles on the human body and the environment, *in vitro* studies that evaluate the nanoparticle toxicity on human cells and *in vitro/in vivo* studies on other living organisms are considered. Further, the machining efficiency of the chosen nanoparticles in the machining industry is highlighted with relevant studies from the literature. The culmination of the results on both the effectiveness of nanofluids in machining and their corresponding toxicity is expected to reveal a better understanding of the sustainability of machining with nanofluids.

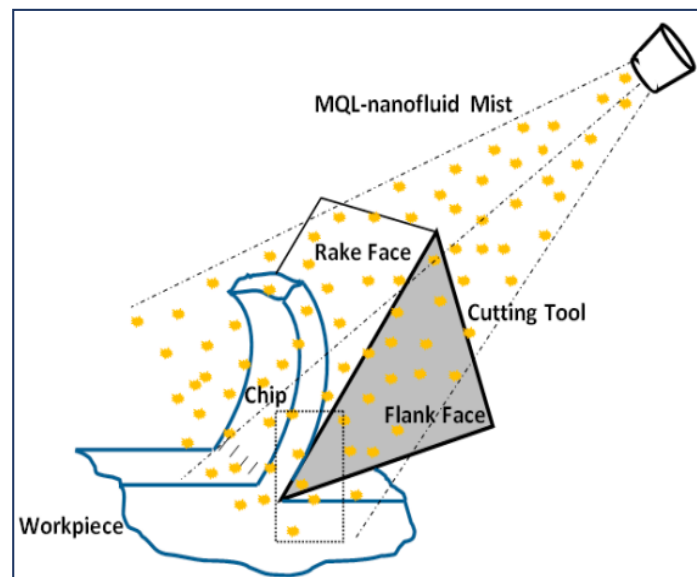


Figure 1. NMQL cooling mechanism [19].

## 2. Research Motivation and Methodology

The literature provides adequate justification towards the positive impact of NMQL cooling strategy in reducing the cutting forces and cutting temperatures in machining. However, the existing research on NMQL machining does not address the toxicity of nanoparticles. This is attributed to a lack of understanding and unavailability of toxicity-related information on nanoparticles. In most cases, research involving nanoparticle toxicity employs very different measurement parameters and therefore makes it very difficult for non-experts to interpret the results. Hence, to completely address the sustainability aspect of NMQL machining, it is important to analyze the toxicity of the nanoparticles before their selection and implementation. Understanding the possible impacts of nanoparticles on human body and other living organisms will motivate researchers to exercise caution in their use. Further, understanding the effect of nanoparticles on the environment (soil and water bodies) will help researchers develop the required disposal plan. The current research aims to address these concerns and develop a review paper on toxicity of nanoparticles used in the machining studies. The results from the available toxicity studies are presented in easily understandable terms and portray the impacts of the nanoparticles on humans, animals, other living organisms and the environment. The review was developed with a focus on clarity of information and ease of understanding. As stated earlier, since the review paper is aimed at aiding researchers in the manufacturing industry, it was important to present the results from toxicity studies in a simple manner but without tarnishing the significance of the data. Following methodology was used in developing this review:

- Review development phase—The review was developed in two stages. In stage one, the effectiveness of NMQL cooling strategy in machining was established from studies available in literature, and six nanoparticles (some nanoparticle families) were chosen for toxicity analysis in stage two of the review. Due to the presence of detailed review papers on NMQL machining's performance, this section of the review was kept brief,

and it highlights only some studies in each of the machining categories. Further, in this section, reference is made to available review papers in current literature on NMQL machining's performance. Stage two focused on building the toxicity review for each of the nanoparticles selected in stage one, and it is the main contribution of this review paper. The following methodology was used for stage two:

1. In vivo and in vitro studies on both human cells and other living organisms were showcased for all nanoparticles. Studies on aquatic life and bacteria helped with estimating the impacts of the nanoparticles on the environment and may help create a safe disposal procedure. Further, in vitro studies on human cells provided information on the possible impacts of working with nanoparticles during the machining process.
  2. The following nanoparticle and toxicity test characteristics were made available from each study: nanoparticle size, nanoparticle concentration in the test medium and duration of exposure to the nanoparticle.
  3. For the development of the toxicity chart, only studies measuring cell viability for seven different human cell lines (human lung epithelial cells (A549), human bronchial epithelial cells (NI-20), AGS human gastric cells, human epidermal cell (HEK), human liver-derived cells (HepG2), human endothelial cells and human peripheral cells) were considered.
- Results communication and dissemination phase—The following considerations were made in presenting the results in this review:
    1. The results from the toxicity studies were presented in table format for each of the selected nanoparticles and in understandable terms.
    2. All studies on each investigated nanoparticle were presented in a chronological order. This was to account for the developing technologies as well as to provide a better insight into some contradictory toxicity results available in the literature.
    3. For the development of the toxicity chart, only studies measuring cell viability for seven different human cell lines (human lung epithelial cells (A549), human bronchial epithelial cells (NI-20), AGS human gastric cells, human epidermal cell (HEK), human liver-derived cells (HepG2), human endothelial cells and human peripheral cells) were considered.

The following sections present the toxicity studies and their results for these selected nanoparticles.

### 3. Toxicity Studies of Nanoparticles

The significance of reducing the amount of lubricant used gave rise to the implementation of MQL techniques, which were then further developed into nano-minimum quantity lubrication. As shown in Table 1, many studies in the literature reflect the positive impacts of introducing nanoparticles in the base oil of a minimum quantity lubrication system. However, the toxicology of the nanoparticles must be understood in order to completely address the sustainability aspect of the machining process with NMQL. Nanoparticles are used in various applications and depending on their usage; nanoparticles may enter the human system by inhalation, oral intake or dermal contact [28,29], as shown in Figure 2.

Nanoparticles' sizes and surface charges determine their reactions with biological fluids, and hence, it is essential to understand the capacity of the body's biological barriers in identifying these contaminants [30]. Studies have shown that smaller nanoparticles travel to the alveolar region and then to the secondary organs, resulting in increased toxicity and causing systemic effects. In contrast, larger particles are likely to be deposited in the upper airways [31,32]. Further, the impacts of nanoparticles on the environment and other living organisms are also important to realize a safe disposal procedure for the nanofluids. Some terminologies relevant to the discussion ahead are detailed below:

- In vitro studies—Toxicity studies conducted outside a living organism. Usually, a cell culture is developed and the nanoparticles are then added to the cell culture for certain durations of time to examine their effects.
- In vivo studies—Toxicity studies conducted by injecting a living organism/animal with a certain dose of nanoparticles. The impacts on the organs/functions of the animal are then studied.
- Cell viability—Cell viability is defined as the number of healthy cells in a sample and can be expressed in percentage. Many studies focus on evaluating concentrations of nanoparticles that reduce the cell viability of a given sample to 50%.
- Cell morphology—Describes the shape, structure, form and size of cells. Changes in cells' morphology might indicate negative impacts on cell function.

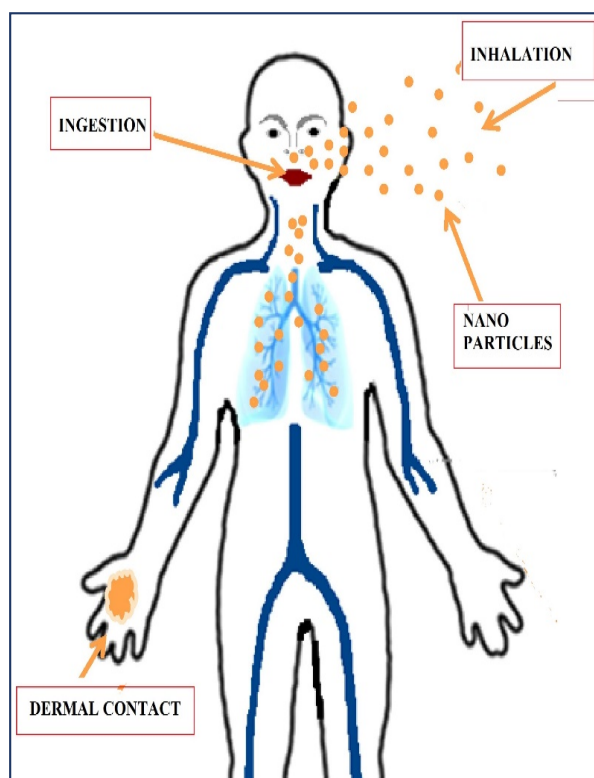


**Figure 2.** Nanoparticle routes of exposure [19].

The following sections present both in vivo and in vitro research on toxicity levels for the selected frequently used nanoparticles.

### 3.1. Molybdenum Disulfide ( $\text{MoS}_2$ )

$\text{MoS}_2$  is one of the important transition-metal dichalcogenides (TMD) with growing applications in the industry. The low friction coefficient of  $\text{MoS}_2$  particles ( $\mu = 0.003$ ) has guaranteed this substance a place as a general application lubricant [33]. In vitro analyses to study the toxicity of  $\text{MoS}_2$ ,  $\text{WS}_2$  and  $\text{WSe}_2$  particles on human lung epithelial cells were conducted by Teo et al. [34]. The study highlighted the relative inertness of transition-metal dichalcogenides when compared to their organic analogs, such as graphene oxide. The viability of the cells was not significantly altered by the addition of  $\text{MoS}_2$  and  $\text{WS}_2$  particles. Furthermore, among the TMDs tested,  $\text{WSe}_2$  resulted in the least cell viability while  $\text{WS}_2$  and  $\text{MoS}_2$  had very low toxicological effects on cells. Table 2 presents the toxicity studies on  $\text{MoS}_2$  particles in the chronological order of publication. The following important observations were made:

- The in vitro studies on human cell lines generally provide a very low toxicity when  $\text{MoS}_2$  nanoparticles are added to cell cultures.

- The method of nanoparticle exfoliation is highlighted as critical in determining the toxicity levels of MoS<sub>2</sub> nanoparticles.
- A study on *Escherichia coli* to study the effects of MoS<sub>2</sub> in natural water provided a high mortality rate. Thus, it indicates a need to be careful in the disposal of the nanoparticles. Further, a lack of in vivo studies on MoS<sub>2</sub> has been noted. This is attributed to the relative newness of MoS<sub>2</sub> nanoparticles when compared to CNT and metal oxides.

**Table 2.** MoS<sub>2</sub> toxicity studies in chronological order.

Type of Study	Concentration	Diameter (nm)	Time of Exposure	Cell Line/Organism	Major Outcomes
In vitro	100 µg/mL		24 h	Human lung epithelial cells	TMDs resulted in a higher cell viability than their organic analogs, such as graphene oxide. Furthermore, among the TMDs tested, WSe <sub>2</sub> resulted in the least cell viability while WS <sub>2</sub> and MoS <sub>2</sub> had very low toxicological effects on the cell [34].
In vitro	0–400 µg/mL		24 h	Human lung carcinoma epithelial cells	The toxicity of the nanoparticle was shown to increase with an increasing degree of exfoliation and was also dependent on the intercalating agents used. MeLi-exfoliated MoS <sub>2</sub> showed the least toxicity [35].
In vitro	0–100 µg/mL	80–100	24 h	Human bronchial cells (NL-20)	The research stated that compared to silica dioxide and carbon black nanoparticles, up to a concentration of 100 µg mL <sup>-1</sup> , WS <sub>2</sub> and MoS <sub>2</sub> nanoparticles exhibited a very low toxicity. At the highest concentration, the cell viability was above 85% for both WS <sub>2</sub> and MoS <sub>2</sub> [36].
In vitro	0.1–100 µg/mL	200–300	48 h	Human epithelial kidney cells (HEK293f)	WS <sub>2</sub> and MoS <sub>2</sub> both exhibited high cell survival rates of over 90% over a 48 h exposure. The authors concluded they are safe for biomedical applications [37].
In vitro	0.5–30 µg/mL	50	24 h	Human hepatoma HepG2 cells	At 30 µg/mL, MoS <sub>2</sub> and BN nanoparticles reduced cell viability [38].
In vitro	0–50 mg/L	50 and 90	4 h	<i>Escherichia coli</i> ( <i>E. coli</i> )	MoS <sub>2</sub> resulted in a mortality rate of 38.5%, while WS <sub>2</sub> caused a mortality rate of 31.2%. The study aimed to research the effects of NPs in natural water under UV irradiation [39].
In vitro	0.1–25 µg/mL	1–1.12	24 h	Human embryonic lung fibroblasts (HELFs).	The cell viability reduced to about 80% at a concentration above 10 µg/mL [40].
In vitro	0.5, 2 and 10 µg/mL	50, 117 and 177	24, 48 and 72 h	Human acute monocytic leukemia (THP-1) Human lung adenocarcinoma (A-549) Human gastric adenocarcinoma (AGS)	The authors concluded that these three sizes of MoS <sub>2</sub> nanoparticles are non-toxic at a concentration of 100 µg mL <sup>-1</sup> in the three cell lines that were studied [30].
In vitro	2.5–200 µg/mL	<100	24, 48 and 72 h	Normal bronchial epithelium cells BEAS-2B (CRL-9609)	MoS <sub>2</sub> NPs and MoS <sub>2</sub> MPs exhibit a similar toxicity. After a 72 h exposure, the cell viability reduced to about 50% at all concentration levels. No dose-dependent increase in toxicity was observed [41].

### 3.2. Tungsten Disulfide (WS<sub>2</sub>)

Similar to MoS<sub>2</sub> nanoparticles, tungsten disulfide (WS<sub>2</sub>) particles are part of the TMD family of 2D nanomaterials and exhibit excellent lubrication properties with a dynamic friction coefficient of 0.03 and a static friction coefficient of 0.07 [42]. Table 3 presents the toxicity studies on WS<sub>2</sub> particles in the chronological order of publication. The following important observations were made:

- Similar to MoS<sub>2</sub> nanoparticles, in vitro studies on human cell lines generally provide a very low toxicity for WS<sub>2</sub> nanoparticles.
- A study on *Escherichia coli* to study the effect of WS<sub>2</sub> in natural water provided a high mortality rate. Additionally, a study on the effects of WS<sub>2</sub> nanoparticles on a fungus also resulted in high levels of toxicity. Therefore, it is essential to develop a safe disposal mechanism to protect the environment from exposure to these nanoparticles.
- Further, both WS<sub>2</sub> and MoS<sub>2</sub> have limited number of in-vivo investigation of their toxicity. This is attributed to the relative newness of TMDs.

**Table 3.** WS<sub>2</sub> toxicity studies in chronological order.

Type of Study	Concentration	Diameter (nm)	Time of Exposure	Cell Line/Organism	Major Outcomes
In vitro	100 µg/mL		24 h	Human lung epithelial cells	TMDs resulted in a higher cell viability than their organic analogs, such as graphene oxide. WSe <sub>2</sub> resulted in the least cell viability while WS <sub>2</sub> and MoS <sub>2</sub> had very low toxicological effects on the cell [34].
In vitro	0–100 µg/mL	80–100	24 h	Human bronchial cells (NL-20)	The research stated that compared to silica dioxide and carbon black nanoparticles, up to a concentration of 100 µg mL <sup>-1</sup> , WS <sub>2</sub> and MoS <sub>2</sub> nanoparticles exhibited a very low toxicity. At the highest concentration, the cell viability was above 85% for both WS <sub>2</sub> and MoS <sub>2</sub> [36].
In vitro	0.22, 3.52 and 35.2 µg/mL	120–150	24 h	Salivary gland cells	The cell viability and cell morphology were unaffected by WS <sub>2</sub> uptakes [43].
In vitro	0.1–100 µg/mL	200–300	48 h	Human epithelial kidney cells (HEK293f)	WS <sub>2</sub> and MoS <sub>2</sub> both exhibited high cell survival rates of over 90% over a 48 h exposure. The authors concluded they are safe for biomedical applications [37].
In vitro	0–50 mg/L	50 and 90	4 h	<i>Escherichia coli</i> ( <i>E. coli</i> )	MoS <sub>2</sub> resulted in a mortality rate of 38.5%, while WS <sub>2</sub> caused a mortality rate of 31.2%. The study aimed to research the effect of NPs in natural water under UV irradiation [39].
In vitro	0–100 µg/mL	≈500	24, 48 and 72 h	Human urinary bladder cells	An 87% cell viability was observed at the highest concentration after a 72 h exposure [44].
In vitro	20–160 mg/L	20–500	24 h	Human A549 cells Fungus <i>Saccharomyces cerevisiae</i>	The viability of A549 cells was unaffected at all tested concentrations. However, the cell vitality of the fungus reduced to about 70% at the highest concentration [45].

### 3.3. Hexagonal Boron Nitride (hBN)

The chemical composition of hBN consists of equal amounts of boron and nitrogen atoms, synthetically manufactured from boric acid (H<sub>3</sub>BO<sub>3</sub>) or boron trioxide (B<sub>2</sub>O<sub>3</sub>). It has very good lubricating properties [46]. Horvath et al. studied the effects of boron nitride nanotubes (BNNT) on human lung alveoli and embryonic kidney cells in an in vitro analysis [47]. It was concluded that boron nitride nanotubes are cytotoxic and their toxicity is greater than that of carbon nanotubes. The authors hypothesized that the increased

toxicity of BNNT could be due to their rod-like structure and highlighted the need for in vivo studies before larger implementations in medical fields. In contrast to Horvath's work, Turco et al. studied the cell viability, cytoskeleton integrity and DNA damage in human vein endothelial cells and reported that BNNT had a non-significant effect on the cells [48]. It was reported that a modest reduction in cell viability occurred at only the highest concentrations ( $100 \mu\text{g mL}^{-1}$ ). Further, Campatelli et al. [49,50], in a direct response to the work by Horvath et al. [47], conducted a further investigation on the toxicity of hBN nanoparticles. The research highlighted that hBN nanoparticles with lengths greater than  $10 \mu\text{m}$  (similar to the ones used in the works of Horvath et al.) produce toxic effects in the cell, while shorter hBN nanoparticles do not exhibit toxic effects on the same cell lines. Table 4 presents the toxicity studies on BN-NT/hBN nanoparticles in the chronological order of publication. The following important observations were made:

- The early literature on hBN provided contradictory results on toxicity. However, further research has highlighted the cause for the discrepancy in results. The lengths of nanoparticles are crucial in determining the particles' toxicity levels.
- In vivo studies on mice showcased a dose-dependent increase in toxicity. Therefore, it is very important to understand the toxicity of hBN nanoparticles relative to their concentration levels.
- Soil worms (*C. elegans*) were impacted by the presence of nanoparticles in their systems. This highlights the need to be cautious in the disposal of the nanoparticles in the environment.
- Study by Xin et al. [51] estimated  $40 \mu\text{g}$  as equal to almost approximately 2–3 decades of work exposure to humans, and  $4 \mu\text{g}$  was estimated to be about 2–7 years of work exposure. Such estimates are important in understanding the safety criteria for the use and implementation of these nanoparticles.

**Table 4.** hBN toxicity studies in chronological order.

Type of Study	Concentration	Diameter (nm)	Time of Exposure	Cell Line/Organism	Major Outcomes
In vitro	$5 \mu\text{g/mL}$ of PEI-BNNT (1:10)		72 h	Human neuroblastoma cell line (SH-SY5Y)	No adverse effects on metabolism, viability or cellular replication were reported. A good cell viability was maintained throughout the test period [49].
In vitro	$2 \mu\text{g/mL}$	<80	48 h	Human lung epithelial cells (A549) alveolar macrophages (RAW 264.7) fibroblast cells (3T3-L1) Human embryonic kidney cells (HEK293)	Shape and geometry are crucial parameters that dictate the toxicity of nanomaterials. BNNT was found to exhibit toxicity to cell lines at low concentrations [47].
In vitro	$0\text{--}100 \mu\text{g/mL}$	75–220	72 h	Human vein endothelial cells (HUVECs)	BNNT had a non-significant effect on the cells. It was reported that a modest reduction in cell viability occurred at only the highest concentrations ( $100 \mu\text{g mL}^{-1}$ ) [48].
In vitro	$0\text{--}100 \mu\text{g/mL}$	10–80	24–48–72 h	Human neuroblastoma SH-SY5Y cells Human umbilical vein endothelial cells (HUVECs)	Both cell lines exhibited a high viability even at high concentrations of $20 \mu\text{g/mL}$ . A shorter BNNT was observed to have a low cytotoxicity when compared to longer nanotubes. The same BNNTs with longer lengths ( $10 \text{ nm}$ ) were found to be toxic at concentrations as low as $2 \mu\text{m}$ [52].

Table 4. Cont.

Type of Study	Concentration	Diameter (nm)	Time of Exposure	Cell Line/Organism	Major Outcomes
In vitro	25 µg/mL		24 h	Human cells	Cell stiffness was calculated using atomic forced microscopy. It was seen that there was no significant change in the cell stiffness before and after hBN uptakes. Therefore, the authors posed it as safe for biomedical use. Further in vivo studies are encouraged [53].
In vitro/in vivo	0–100 µg/mL and 40 µg	49	24 h	NLRP3-deficient human monocytic cells C57BL/6 J male mice	Both in vitro and in vivo studies resulted in acute inflammation and toxicity due to BNNT contaminations [54].
In vitro	0–20 µg/mL	<50		Human hepatoma HepG2	At 30 µg/mL, MoS <sub>2</sub> and BN nanoparticles reduced cell viability [38].
In vivo	1–500 µg/mL	150	0–30 days	<i>Caenorhabditis elegans</i> ( <i>C. elegans</i> )	It was seen that up to a concentration of 100 µg mL <sup>-1</sup> , BNNTs did not cause any significant alteration to the growth, locomotion, lifespan or progeny of the <i>C. elegans</i> nematodes. However, at concentrations over 100 µg mL <sup>-1</sup> , BNNTs significantly reduced growth and locomotion and affected other characteristics [55].
In vitro	0.025–0.4 mg/mL	50–190	24 and 48 h	Human normal skin fibroblast (CCD-1094Sk and ATCC <sup>®</sup> CRL 2120 <sup>TM</sup> ) Madin–Darby canine kidney (MDCK) cells	At a low concentration of 0.025–0.1 mg/mL, no cytotoxicity was observed. However, at concentrations over 0.2 mg/mL, a mild cytotoxicity was noted on CRL-2120 cells. The authors concluded that at concentrations below 0.1 mg/mL, hBN can be a safe oral care product [56].
In vivo	4 and 40 µg	13–23	4 h 1–7 days 1–2 months	Male C57BL/6 J mice	A concentration of 40 µg caused the greatest amount of damage to the lungs. 40 µg was estimated as equal to almost approximately 2–3 decades of work exposure to humans. 4µg was estimated to be about 2–7 years of work exposure, but resulted in no toxicity [51].
In vivo	50–3200 µg/kg	50–200	24 h	Wistar albino rats	At concentrations below 1600 µg/kg, no toxicity was observed. Concentrations of 1600 µg/kg and 3200 µg/kg caused significant damage to the liver [57].

### 3.4. Aluminum Oxide (AL<sub>2</sub>O<sub>3</sub>)

Metallic oxide nanoparticles have various applications within the industry due to their physical and chemical properties, such as transparency, high isoelectric effects and photocatalytic efficiency [58]. AL<sub>2</sub>O<sub>3</sub> also exhibits a resistance to chemical corrosion [59]. Weisheng et al. compared the cytotoxicity of AL<sub>2</sub>O<sub>3</sub> nanoparticles on human bronchioloalveolar carcinoma cells (A549) with that of titanium dioxide (TiO<sub>2</sub>) and cerium oxide (CeO<sub>2</sub>) [60]. The A549 cell viability was unaffected up to a concentration of 5 µg mL<sup>-1</sup>; however, at dosages of 10 µg mL<sup>-1</sup> and 25 µg mL<sup>-1</sup>, the cell viability was reduced to 86% and 82.8%, respectively. It was determined that CeO<sub>2</sub> caused the cell viability to be reduced to 68.3% at 25 µg mL<sup>-1</sup>, while TiO<sub>2</sub> resulted in a cell viability of 89.3% at the maximum concentration of 25 µg mL<sup>-1</sup>. The level of toxicity was determined to decrease in the following order: CeO<sub>2</sub> > AL<sub>2</sub>O<sub>3</sub> > TiO<sub>2</sub>. Noguiera et al. experimentally analyzed the effects of different

crystalline forms of  $Al_2O_3$  on mouse neuroblastoma cells (N2A) and human bronchial epithelial cells (BEAS-2B) [61]. The two crystalline forms that were studied—alpha  $Al_2O_3$  ( $\alpha-Al_2O_3$ ), which has a hexagonal structure, and eta  $Al_2O_3$  ( $\eta-Al_2O_3$ )—revealed different toxicology results. This gives strength to the hypothesis that the crystalline forms influence the nanoparticle toxicity. Both  $\alpha$  and  $\eta-Al_2O_3$  resulted in a decreased cell viability in both N2A and BEAS-2B cells with the latter crystalline form showing a greater toxicity. The decrease in cell viability was dependent on both the concentrations and the durations of cell exposure to these NPs. Table 5 represents the toxicity studies on  $Al_2O_3$  nanoparticles in the chronological order of publication. The following important observations were made:

- $Al_2O_3$  nanoparticles are relatively less toxic when compared to other metal oxides, such as ZnO and  $SiO_2$ .
- Dose-dependent increases in toxicity were observed. Low concentrations of  $Al_2O_3$  nanoparticles of up to  $100 \mu g/mL^{-1}$  resulted in low toxicity levels in human cell lines. However, in fish cells, higher toxicity levels were observed for the same levels of nanoparticle concentration.
- In vivo studies on mice also showcased inflammation and damage to the liver.

**Table 5.**  $Al_2O_3$  toxicity studies in chronological order.

Type of Study	Concentration	Diameter (nm)	Time of Exposure	Cell Line/Organism	Major Outcomes
In vitro	10–100 $\mu g/mL$	40–47	48 h	Mouse neuroblastoma (neuro-2A)	The cell viability was unaffected at concentrations up to $100 \mu g/mL^{-1}$ during a 48 h exposure [62].
Aqueous suspension	0.1–50 mg/L	80	96 h	Zebrafish larvae/embryo	Even at the highest concentrations, no effect on hatching rate or survival was observed. The effect was non-toxic [63].
In vitro	1 $\mu M$ –10 mM	8	24 h	Human brain microvascular endothelial cells (HBMEC)	It resulted in low cell viability of 20% at a concentration of 10 mM. No change in viability was observed for up to 0.01 mM [64].
In vivo	29 mg/Kg b.w.	8	24 h	Fisher 344 rats	It resulted in alterations of mitochondrial functions and decreased expression of tight junction proteins [64].
In vitro	1–250 $\mu g/mL$	10–20	8 h	Porcine pulmonary artery endothelial cells/human umbilical vein endothelial cells	Inflammation was observed. The results indicated a probable cardiovascular disease risk [65].
Aqueous suspension	3–192 mg/L	50	72 h	<i>Scenedesmus</i> sp./ <i>Chlorella</i> sp.	A 50% mortality rate was observed for <i>Chlorella</i> at 45.4 mg/L and 39.35 mg/L for <i>Scenedesmus</i> [66].
Aqueous suspension	5–100 mg/L	5 and 50	24 and 96 h	<i>Artemia salina</i> (crustacean filter feeder) larvae	$\gamma-Al_2O_3$ NPs were more toxic than $\alpha-Al_2O_3$ NPs at all concentrations. The highest mortality rate of 34% was observed at 100 mg/L for a 96 h exposure [67].
Aqueous suspension	0.005–3.8 mg/L	20	72 h	Green micro-algae <i>Dunaliella salina</i>	A swelling and enlargement of <i>Dunaliella</i> cells was observed. It resulted in a significant impact on the shape and topography [68].
In vitro	10–100 $\mu g/mL$	50	6, 12 and 24 h	Chinook salmon (CHSE-214)	A dose-dependent reduction in cell viability was observed. At 10 $\mu g/mL$ , the cell viability was found to be 80%, while at 100 $\mu g/mL$ , it was about 60% for a 24 h exposure [69].

Table 5. Cont.

Type of Study	Concentration	Diameter (nm)	Time of Exposure	Cell Line/Organism	Major Outcomes
In vivo	1.5, 3 and 6 mg/kg b.w.	50	13 weeks	ICR mice	The kidney, liver and immune systems were impacted. There was a development of a pathological lesion in the kidney and liver [70].
In vitro	100 µg/L	39.4	24 h	Human lymphocytes	AL <sub>2</sub> O <sub>3</sub> did not cause DNA damage when compared to other metal oxide NPs (Co <sub>3</sub> O <sub>4</sub> , Fe <sub>2</sub> O <sub>3</sub> and SiO <sub>2</sub> ) studied [71].
In vivo	10 and 100 µg/L	20	7, 14 and 21 days	Freshwater fish ( <i>Carassius auratus</i> )	Liver degeneration and gill hyperplasia were observed when exposed to both aluminium oxide and ZnO nanoparticles [72].
In vivo	120–300 ppm		96 h	Freshwater fish <i>Oreochromis mossambicus</i>	A 50% mortality rate was observed at a concentration of about 235–245 ppm. Accumulations of NPs were found in the fish liver, affecting the health conditions of the fish [73].
In vitro	1–2000 ppm	19.8	72 h	Human peripheral blood lymphocytes	No genotoxicity was observed in the cells even at the highest concentration [74].
In vivo	0–5 mg/m <sup>3</sup>	11.94	28 days	Sprague Dawley rats	Lungs were the most impacted organ. An alveolar macrophage accumulation was found in the lungs. The level of no observed adverse effects of AL <sub>2</sub> O <sub>3</sub> NPs in male rats was suggested to be about 1 mg/m <sup>3</sup> [75].
In vivo	70 mg/kg b.w.	50	75 days	Wistar male albino rats	Liver and kidney damage were observed in the rats. A weight reduction occurred when compared to a control group without nanoparticle injections [76].
In vivo	70 mg/kg b.w.	50	75 days	Wistar male albino rats	It caused changes on the testicular architecture and caused fertility problems through different pathways, including cell death and oxidative stress [77].
In vivo	0.1 and 1 mM	50	Lifespan—chronic exposure	Flies— <i>Drosophila melanogaster</i>	Wing blisters, malformed legs and a segmented thorax were observed in progeny flies. Behavioural defects in climbing were also noticed [78].
Aqueous suspension	0–500 mg/L	50	96 h	Zebrafish larvae	At a concentration of 130 mg/L, 50% of the larvae died. It was also noted that at sub-lethal concentrations, AL <sub>2</sub> O <sub>3</sub> -NPs can produce DNA damage and change stress-related gene expressions in zebrafish larvae [79].

### 3.5. Zinc Oxide (ZnO)

The metallic oxide of zinc is used in many applications, including cosmetics for protection against UV rays [62]. Weisheng et al. investigated the toxicity of ZnO nanoparticles on human lung epithelial cells. This study found that there was a 75–85% decrease in cell viability between concentrations of 18 and 25 µg mL<sup>-1</sup>, respectively [80]. The authors reported a steep decline in cell viability for ZnO compared to the NPs of other metallic oxides. This observation was supported by Qiang et al. in a comparative study of different metallic oxides [59]. ZnO resulted in the greatest decrease in cell viability when compared to metallic oxides of aluminum, silica and titanium. Sliwinska et al. further confirmed the non-biocompatibility of ZnO nanoparticles with human peripheral blood lymphocytes [58]. Table 6 represents the

toxicity studies on ZnO nanoparticles in the chronological order of publication. The following important observations were made:

- High levels of toxicity were observed at even low concentrations within in vitro cytotoxicity studies on human cell lines.
- In vivo studies also showcased high levels of toxicity and damage to the liver.

**Table 6.** ZnO toxicity studies in chronological order.

Type of Study	Concentration	Diameter (nm)	Time of Exposure	Cell Line/Organism	Major Outcomes
In vitro	10–100 µg/mL	50–70	48 h	Mouse neuroblastoma (neuro-2A)	Cell viability was unaffected at concentrations below 25 µg/mL. At higher concentrations, 15–50% of the cells died during a 48 h exposure. Mitochondrial function was also severely impacted [62].
In vitro	0–30 ppm and 0–15 ppm		3–6 days	Human mesothelioma/rodent fibroblast cell	Above 15 ppm, all cells died over a 3 day exposure to ZnO nanoparticles [81].
Aqueous suspension	0.1–0.16 mg/L	50–70	72 h	Algae— <i>Pseudokirchneriella subcapitata</i>	Algae growth inhibition was observed at 0.1 mg/L. Total growth observation occurred at 0.16 mg/L [82].
Aqueous suspension	0.1–50 mg/L	20	96 h	Zebrafish larvae/embryo	At concentrations less than 0.5 mg/L, no toxicity was observed. At higher concentrations, a dose-dependent increase in toxicity on survival and hatching rate was recorded [63].
In vitro	31.25–1000 mg/L	50–70	16–18 h	Yeast— <i>Saccharomyces cerevisiae</i>	An 80% inhibition of growth occurred at 250 mg/L [83].
In vitro	5–100 µg/mL	50	24 h	Human hepatocyte cell (L02)/human embryonic kidney cell (HEK293)	Reduced mitochondrial function occurred at concentrations of 10 µg/mL. ZnO resulted in DNA damage, cell membrane disruption and subsequent cell death [84].
In vivo	5–2000 mg/kg body weight	20	14 days	Sprague Dawley rats	Toxicity was observed at low doses. Higher liver damage was observed at low does of 5 mg/kg b.w. compared to 2000 mg/kg b.w. Cell inflammation and clotting were observed [85].
In vivo	125–250–500 mg/kg of body weight	20	90 days	Sprague Dawley rats	The pancreas, eye and stomach were affected at a low concentration of 125 mg/kg b.w. At 250 and 500 mg/kg b.w., significant changes in terms of anemia in the hematological and blood chemical analysis occurred [86].
In vivo	10/100 µg/L	50	7/14/21 days	Freshwater fish ( <i>Carassius auratus</i> )	Liver degeneration and gill hyperplasia were observed when exposed to both aluminium oxide and ZnO nanoparticles [72].
In vitro	1–2000 ppm	19.8	72 h	Human peripheral blood lymphocytes	Genotoxicity was observed at even a low concentration of 12.5 ppm. A high concentration of 500 ppm resulted in a mortality of blood cells [74].
In vivo	100 mg/kg b.w.	100	75 days	Wistar male albino rats	Liver and kidney damage were observed in the rats. A weight reduction occurred when compared to a control group without nanoparticle injections [76].
In vivo	100 mg/kg b.w.	100	75 days	Wistar male albino rats	ZnO caused changes to the testicular architecture and caused fertility problems through different pathways, including cell death and oxidative stress [77].

### 3.6. Carbon Nanotubes (CNT, SWCNT and MWCNT)

Carbon nanotubes, due to their excellent structural, mechanical, electrical and optical properties, are used in many industrial applications. A good amount of literature exists on the toxicity levels of CNTs due to their longer presence in the industry. An in vivo toxicity study on mice comparing CNTs to asbestos observed that CNTs result in the formation of a scar-like structure (lesion) similar to asbestos that is a carcinogenic. Table 7 represents

the toxicity studies on CNT nanoparticles in the chronological order of publication. The following important observations were made:

- High levels of toxicity were observed at even low concentrations within in vitro cytotoxicity studies on human cell lines. Some contradictory results are also available in the literature.
- In vivo studies highlighted short-term impairments of fear, memory and morphological changes and an increased heartbeat.

**Table 7.** CNT toxicity studies in chronological order.

Type of Study	Concentration	Diameter (nm)	Time of Exposure	Cell Line/Organism	Major Outcomes
In vitro	1.56–800 µg/mL	0.8–1.2	24 h	A549 human lung cell	A significant cytotoxicity was recorded at concentrations above 400 µg/mL [87].
In vitro	0.05 µg/mL–0.05 mg/mL	1	24 and 48 h	Human epidermal keratinocytes (HEKs)	A low concentration of 0.05 µg/mL maintains cell viability. A dose-dependent decrease in cell viability was observed. At a high concentration of 0.05 mg/mL, cell viability was reduced to about 50% during a 48 h exposure [88].
In vivo	50 µg	15–100	24 h	Mice	Similar to asbestos, MWCNTs result in the formation of a scar-like structure (lesion) called granuloma. Great caution is advised in the use of CNTs [89].
In vivo	2 mg/1.5 mL/b.w.	15–25	1–144 h	Male Wistar rats	MWCNT translocates progressively in the spleen, with a peak of concentration after 48 h. Transient alterations due to oxidative stress and inflammation were present and need further investigation [90].
In vitro	3–300 µg/mL	60–300	48 h	Human embryonic kidney cell line (HEK293)	A 50% reduction in cell viability was observed at 87.58 µg/mL. A dose-dependent increase in cell membrane damage was observed at 10–100 µg/mL [91].
In vivo	0.5, 1 and 2.1 mg/mL	100	24 h and 30 min	Male Wistar rats	It caused a short-term impairment in fear memory retrieval. However, the effect was transient and overcome in 24 h [92].
In vivo	4 mg/kg b.w.		7 days	Male BALB/c mice	The organ coefficient and GSH levels in the brain and kidney decreased when compared to a control group. Morphological changes were also seen in the experimentation [93].
In vivo	1 mg/kg b.w.	5–10	0.5 h	Male Wistar rats	An increased heart rate was observed in rats after injections of CNTs. A possible blockage of potassium channels may be the cause [94].

#### 4. Discussion

MQL is a mist lubrication strategy, and hence, it has a high probability of resulting in airborne impurities, such as nanoparticles. This review details the toxicity of six nanoparticles frequently used in nano-MQL machining. From the available literature, it is evident that nanoparticles improve machining performance. However, they also impact human health and the environment. Therefore, it is critical for researchers and workers experimenting in the use of NPs in the machining sector to be cautious regarding the handling, preparation and operation of nanofluids. The most frequently used nanoparticles in the machining

studies available in the literature are identified as tungsten disulfide ( $WS_2$ ), molybdenum disulfide ( $MoS_2$ ), boron nitride (BNNT and hBN), carbon nanotubes (CNT, SWCNT and MWCNT) and oxides of zinc (ZnO) and aluminum ( $Al_2O_3$ ).  $MoS_2$  nanoparticle additives improve the machining performance in minimum quantity lubrication machining. In a comparative study with different nanoparticles,  $MoS_2$  performed the best with a low surface roughness and lower cutting forces [13]. The machining performance of  $WS_2$  was also comparable to that of  $MoS_2$ . The toxicity studies for  $MoS_2$  and  $WS_2$  nanoparticles presented in Tables 2 and 3, respectively, attest the very low toxicity of TMDs ( $MoS_2$  and  $WS_2$ ). Therefore, the high machining performance and low toxicity present TMDs as an ideal choice for nano-minimum quantity lubrication. However, important observations from the toxicity studies on  $MoS_2$  indicate that the method of manufacturing affects their toxicity. Further,  $WS_2$  nanoparticles exhibit toxicity in natural water and affect fungi growth. The experimental investigations for  $MoS_2$  and  $WS_2$  listed in Table 1 do not provide details related to their methods of manufacturing or the disposal mechanisms employed. This review highlights the need for researchers to clearly indicate these parameters to achieve a proper sustainability analysis.

The toxicity of hBN nanoparticles varies depending on the length. A high toxicity is observed at larger lengths, while very low toxicity levels are seen at shorter lengths. Additionally, the chronological presentation of toxicity studies on hBN nanoparticles show the development of a consensus regarding how the lengths of nanotubes effect their toxicity. However, in vivo studies presented some concerning results on the impacts of hBN nanoparticles over certain concentrations. The in vivo study conducted on *C. elegans* showcased the detrimental effects on the growth, the locomotion and the progeny of these nematodes [55]. Although the results are not analogous to humans, it does raise important questions regarding possible similarities in its toxicity on the human body. The NMQL machining studies with hBN additives provided a good machining performance. However, due to few alarming toxicity results present in the literature, care must be taken in the selection of hBN nanoparticles. If the use of hBN nanoparticles cannot be avoided, particles with short lengths must be used. Similar to hBN nanoparticles, the toxicity of  $Al_2O_3$  is affected by its crystalline structures.  $\gamma$ - $Al_2O_3$  NPs were more toxic than  $\alpha$ - $Al_2O_3$  NPs at all concentrations. Therefore, researchers need to avoid the use  $\gamma$ - $Al_2O_3$  nanoparticles. ZnO exhibits a very strong toxicity and must be avoided in machining studies. Similarly, carbon nanotubes have been seen to form lesions similar to the effects of asbestos.

For a quick and easy understanding of the toxicity levels of the chosen nanoparticles, an attempt was made to develop a chart that maps the toxicity levels of the nanoparticles on seven different human cell lines representing the possible exposure routes of nanoparticles. Many researchers have used human lung epithelial cells (A549) for toxicity studies representing exposure to inhaled nanoparticles. Bronchial epithelial cells (NL-20) have also been used. The effects of nanoparticle ingestion have been represented by using in vitro toxicity studies on human gastric cell lines (AGS), human epidermal keratinocytes (HEKs) and human liver-derived cells (HepG2), while blood-related toxicity has been represented by using in vitro studies on human peripheral blood cells and human endothelial cells. Cell viability is defined as the number of healthy cells in a sample [95] and was used as a marker to establish the comparison chart seen in Table 8. It must be noted that all studies seen in the toxicity studies of individual nanoparticles were not included in the chart. In order to facilitate a comparison, only in vitro studies on select human cell lines were included in the chart. The cell viability marker is represented as a percentage and provides an easy understanding of the toxicity levels for each nanoparticle.

**Table 8.** Comparison of nanoparticle toxicities on human cells.

In Vitro Toxicity Test Parameters			Nanoparticle Exposure Route					
Nanoparticle	Exposure (h)	Concentration	Inhalation		Ingestion		Dermal	
			A549 Human Lung Epithelial Cells	NL-20 Human Bronchial Epithelial Cells	AGS Human Gastric Cells	Human Epidermal Keratinocytes (HEKs)	HepG2 Human Liver-Derived Cells	Human Endothelial Cells
Cell Viability %								
MoS <sub>2</sub>	24	100 µg mL <sup>-1</sup>	87%					[34]
	24	100 µg mL <sup>-1</sup>	70–95%					[35]
	24	10 µg mL <sup>-1</sup>		98%		98–100%		[36]
	24	10 µg mL <sup>-1</sup>	>90%		<50%			[30]
WS <sub>2</sub>	24	85%						[34]
	24		90%			98–100%		[36]
hBN	120	20 µg mL <sup>-1</sup>	30%					[47]
	72	20 µg mL <sup>-1</sup>					100%	[50]
AL <sub>2</sub> O <sub>3</sub>	24	10 mM						70%
	24	25 µg mL <sup>-1</sup>	80%					[47] [60]
ZnO	24	10 mM						44%
	24	18 µg mL <sup>-1</sup>	20%					[58] [80]
CNT	24	0.05 mg/mL				50%		[88]
	48	87.58 µg mL <sup>-1</sup>				50%		[91]

## 5. Conclusions

The literature on machining with NMQL does not explicitly address the safety aspect of dealing with nanoparticles. This study is an attempt to bridge that gap in the literature by providing the toxicity details regarding the most-used nanoparticles in machining. The review includes both in vivo and in vitro studies assessing the toxicity of the nanoparticles on human cells and other organisms. This will allow researchers to understand the impacts of nanoparticles on human health as well as on the environment and thereby devise appropriate methodologies for the safe handling and disposal of these nanoparticles. Further, for the easy assessment of toxicity levels, a toxicity chart for nanoparticles was developed. Cell viability measured from in vitro toxicity studies of nanoparticles on seven different cell lines representing three possible exposure routes (inhalation, ingestion and dermal contact) was used as a marker to establish the visual representation found in Table 8. This table compares the toxicity of six different nanoparticles used in NMQL machining processes. The following conclusions have been drawn from this review:

- Transition metal dichalcogenides (MoS<sub>2</sub> and WS<sub>2</sub>) exhibit a very low toxicity when compared to other nanoparticles and provide a very good machining performance with a good surface finish and lower cutting forces. Among the MoS<sub>2</sub> and WS<sub>2</sub> nanoparticles, MoS<sub>2</sub> provides a better surface finish and exhibits a lower toxicity. However, a lack of in vivo studies and the relative infancy of the toxicity research on these nanoparticles must be considered.
- The toxicity of hBN nanoparticles varies depending on the length. A high toxicity was observed at larger lengths, while very low toxicity levels are seen at shorter lengths. Hence, machining with hBN nanoparticles must be done with only short hBN nanoparticles. Similarly, care must be taken in the selection of AL<sub>2</sub>O<sub>3</sub> nanoparticles. The toxicity of AL<sub>2</sub>O<sub>3</sub> nanoparticles varies depending on their crystalline structures but generally exhibits a low toxicity on human cells. However, results from in vivo studies of both hBN and AL<sub>2</sub>O<sub>3</sub> highlight the concern and the need to accurately understand the importance of nanoparticle concentrations.
- ZnO exhibited very high levels of toxicity in both in vitro and in vivo studies, and therefore, irrespective of machining performance, researchers must avoid their use in machining operations. In vivo studies for carbon nanotube toxicity predicted a high toxicity, while in vitro toxicity studies provided contradictory results.

- Some nanoparticles for the same concentration exhibited a higher toxicity in non-human species. This provides researchers information to develop disposal guidelines and highlights the need for the proper disposal of nanofluids after machining.
- The comparisons developed in Table 8 provide an easy interpretation of the toxicity levels of the six nanoparticles that were considered. Cell viability is an important marker for toxicity studies and provides easy interpretations. However, a lack of uniformity in nanoparticle concentrations and the methods employed are limitations. Future research can aim to develop the chart with consistent nanoparticle concentrations and same methods of toxicity analyses.

This is the first attempt to combine the results of the experimental investigations of nano-MQL cooling and the toxicity studies of nanoparticles, allowing researchers to make informed decisions in the selection of the most sustainable nanoparticles in the nano-MQL machining process. Simulation studies enable researchers to understand key parameters, such as temperature changes, heat transfer coefficients, cutting forces and the effects of jet radius and location [96]. The relative difficulty of establishing a realistic model to simulate the effects of nano-minimum quantity lubrication is another reason experimental investigations are unavoidable. The development of CFD and FEM models to simulate nanofluid lubrication to minimize experimentation must be considered and is a topic of future study.

**Author Contributions:** Literature, I.N. and A.E.; writing—original draft preparation, I.N. and A.E.; writing—review and editing, S.P.; visualization, I.N.; supervision, I.D.; funding acquisition, I.D. All authors have read and agreed to the published version of the manuscript.

**Funding:** This research was funded by the Natural Sciences and Engineering Research Council of Canada (NSERC).

**Institutional Review Board Statement:** Not applicable.

**Informed Consent Statement:** Not applicable.

**Data Availability Statement:** Not applicable.

**Acknowledgments:** The authors acknowledge the support provided by the NSERC.

**Conflicts of Interest:** The authors declare no conflict of interest.

## References

1. Black, J.T.; Kohser, R.A. *DeGarmo's Materials and Processes in Manufacturing*, 10th ed.; John Wiley & Sons: Hoboken, NJ, USA, 2008.
2. Dixit, U.S.; Sarma, D.K.; Davim, J.P. *Environmentally Friendly Machining*; Springer: Berlin/Heidelberg, Germany, 2012.
3. Boswell, B.; Islam, M.N.; Davies, I.J.; Ginting, Y.R.; Ong, A.K. A review identifying the effectiveness of minimum quantity lubrication (MQL) during conventional machining. *Int. J. Adv. Manuf. Technol.* **2017**, *92*, 321–340. [[CrossRef](#)]
4. Dureja, J.S.; Singh, R.; Singh, T.; Singh, P.; Dogra, M.; Bhatti, M.S. Performance evaluation of coated carbide tool in machining of stainless steel (AISI 202) under minimum quantity lubrication (MQL). *Int. J. Precis. Eng. Manuf. Green Technol.* **2015**, *2*, 123–129. [[CrossRef](#)]
5. Carou, D.; Rubio, E.M.; Davim, J.P. A note on the use of the minimum quantity lubrication (MQL) system in turning. *Ind. Lubr. Tribol.* **2015**, *67*, 256–261. [[CrossRef](#)]
6. Klocke, F.; Eisenblätter, G. Dry cutting—State of research. *VDI Ber.* **1998**, *46*, 159–188.
7. Tschätsch, H. *Applied Machining Technology*; Springer: Berlin/Heidelberg, Germany, 2009; pp. 5–23. [[CrossRef](#)]
8. Sarikaya, M.; Yilmaz, V.; Güllü, A. Analysis of cutting parameters and cooling/lubrication methods for sustainable machining in turning of Haynes 25 superalloy. *J. Clean. Prod.* **2016**, *133*, 172–181. [[CrossRef](#)]
9. Sharma, A.K.; Tiwari, A.K.; Dixit, A.R. Effects of Minimum Quantity Lubrication (MQL) in machining processes using conventional and nanofluid based cutting fluids: A comprehensive review. *J. Clean. Prod.* **2016**, *127*, 1–18. [[CrossRef](#)]
10. Saidur, R.; Leong, K.Y.; Mohammad, H.A. A review on applications and challenges of nanofluids. *Renew. Sustain. Energy Rev.* **2011**, *15*, 1646–1668. [[CrossRef](#)]
11. Sharma, A.K.; Tiwari, A.K.; Dixit, A.R. Progress of Nanofluid Application in Machining: A Review. *Mater. Manuf. Process.* **2015**, *30*, 813–828. [[CrossRef](#)]
12. Zhang, Y.; Li, C.; Jia, D.; Zhang, D.; Zhang, X. Experimental evaluation of MoS<sub>2</sub> nanoparticles in jet MQL grinding with different types of vegetable oil as base oil. *J. Clean. Prod.* **2015**, *87*, 930–940. [[CrossRef](#)]

13. Kumar, A.; Ghosh, S.; Aravindan, S. Experimental investigations on surface grinding of silicon nitride subjected to mono and hybrid nanofluids. *Ceram. Int.* **2019**, *45*, 17447–17466. [[CrossRef](#)]
14. Viridi, R.L.; Chatha, S.S.; Singh, H. Experiment evaluation of grinding properties under Al<sub>2</sub>O<sub>3</sub> nanofluids in minimum quantity lubrication. *Mater. Res. Express* **2019**, *6*, 096574. [[CrossRef](#)]
15. Eltaggaz, A.; Hegab, H.; Deiab, I.; Kishawy, H.A. Hybrid nano-fluid-minimum quantity lubrication strategy for machining austempered ductile iron (ADI). *Int. J. Interact. Des. Manuf.* **2018**, *12*, 1273–1281. [[CrossRef](#)]
16. Eltaggaz, A.; Zawada, P.; Hegab, H.A.; Deiab, I.; Kishawy, H.A. Coolant strategy influence on tool life and surface roughness when machining ADI. *Int. J. Adv. Manuf. Technol.* **2018**, *94*, 3875–3887. [[CrossRef](#)]
17. Eltaggaz, A.; Nouzil, I.; Deiab, I. Machining ti-6al-4v alloy using nano-cutting fluids: Investigation and analysis. *J. Manuf. Mater. Process.* **2021**, *5*, 42. [[CrossRef](#)]
18. Uysal, A. Investigation of flank wear in mql milling of ferritic stainless steel by using nano graphene reinforced vegetable cutting fluid. *Ind. Lubr. Tribol.* **2016**, *68*, 446–451. [[CrossRef](#)]
19. Nguyen, T.K.; Do, I.; Kwon, P. A tribological study of vegetable oil enhanced by nano-platelets and implication in MQL machining. *Int. J. Precis. Eng. Manuf.* **2012**, *13*, 1077–1083. [[CrossRef](#)]
20. Yıldırım, Ç.V.; Sarıkaya, M.; Kıvak, T.; Şirin, Ş. The effect of addition of hBN nanoparticles to nanofluid-MQL on tool wear patterns, tool life, roughness and temperature in turning of Ni-based Inconel 625. *Tribol. Int.* **2019**, *134*, 443–456. [[CrossRef](#)]
21. Yıldırım, Ç.V. Experimental comparison of the performance of nanofluids, cryogenic and hybrid cooling in turning of Inconel 625. *Tribol. Int.* **2019**, *137*, 366–378. [[CrossRef](#)]
22. Chetan; Ghosh, S.; Rao, P.V. Comparison between sustainable cryogenic techniques and nano-MQL cooling mode in turning of nickel-based alloy. *J. Clean. Prod.* **2019**, *231*, 1036–1049. [[CrossRef](#)]
23. Şirin, Ş.; Kıvak, T. Performances of different eco-friendly nanofluid lubricants in the milling of Inconel X-750 superalloy. *Tribol. Int.* **2019**, *137*, 180–192. [[CrossRef](#)]
24. Said, Z.; Gupta, M.; Hegab, H.; Arora, N.; Khan, A.M.; Jamil, M.; Bellos, E. A comprehensive review on minimum quantity lubrication (MQL) in machining processes using nano-cutting fluids. *Int. J. Adv. Manuf. Technol.* **2019**, *105*, 2057–2086. [[CrossRef](#)]
25. Cui, X.; Li, C.; Ding, W.; Chen, Y.; Mao, C.; Xu, X.; Liu, B.; Wang, D.; Li, H.N.; Zhang, Y.; et al. Minimum quantity lubrication machining of aeronautical materials using carbon group nanolubricant: From mechanisms to application. *Chin. J. Aeronaut.* **2021**. [[CrossRef](#)]
26. Zhang, Y.; Li, H.N.; Li, C.; Huang, C.; Hafiz Muhammad, A.; Xu, X.; Mao, C.; Ding, W.; Cui, X.; Yang, M.; et al. Nano-enhanced biolubricant in sustainable manufacturing: From processability to mechanisms. *Friction* **2022**, *10*, 803–841. [[CrossRef](#)]
27. Pereira, O.; Martín-Alfonso, J.E.; Rodríguez, A.; Calleja-Ochoa, A.; Fernández-Valdivielso, A.; Lopez de Lacalle, L.N. Sustainability analysis of lubricant oils for minimum quantity lubrication based on their tribo-rheological performance. *J. Clean. Prod.* **2017**, *164*, 1419–1429. [[CrossRef](#)]
28. Bergin, I.L.; Witzmann, F.A. Nanoparticle toxicity by the gastrointestinal route: Evidence and knowledge gaps. *Int. J. Biomed. Nanosci. Nanotechnol.* **2013**, *3*, 163. [[CrossRef](#)]
29. Buzea, C.; Pacheco, I.I.; Robbie, K. Nanomaterials and nanoparticles: Sources and toxicity. *Biointerphases* **2007**, *2*, MR17–MR71. [[CrossRef](#)]
30. Moore, C.; Movia, D.; Smith, R.J.; Hanlon, D.; Lebre, F.; Lavelle, E.C.; Byrne, H.J.; Coleman, J.N.; Volkov, Y.; McIntyre, J. Industrial grade 2D molybdenum disulphide (MoS<sub>2</sub>): An in vitro exploration of the impact on cellular uptake, cytotoxicity, and inflammation. *2D Mater.* **2017**, *4*, 025065. [[CrossRef](#)]
31. Oberdörster, G.; Sharp, Z.; Atudorei, V.; Elder, A.; Gelein, R.; Kreyling, W.; Cox, C. Translocation of inhaled ultrafine particles to the brain. *Inhal. Toxicol.* **2004**, *16*, 437–445. [[CrossRef](#)]
32. Braakhuis, H.M.; Gosens, I.; Krystek, P.; Boere, J.A.F.; Cassee, F.R.; Fokkens, P.H.B.; Post, J.A.; Van Loveren, H.; Park, M.V.D.Z. Particle size dependent deposition and pulmonary inflammation after short-term inhalation of silver nanoparticles. *Part. Fibre Toxicol.* **2014**, *11*, 49. [[CrossRef](#)]
33. Mak, K.F.; Lee, C.; Hone, J.; Shan, J.; Heinz, T.F. Atomically thin MoS<sub>2</sub>: A new direct-gap semiconductor. *Phys. Rev. Lett.* **2010**, *105*, 136805. [[CrossRef](#)] [[PubMed](#)]
34. Teo, W.Z.; Chng, E.L.K.; Sofer, Z.; Pumera, M. Cytotoxicity of exfoliated transition-metal dichalcogenides (MoS<sub>2</sub>, WS<sub>2</sub>, and WSe<sub>2</sub>) is lower than that of graphene and its analogues. *Chem. A Eur. J.* **2014**, *20*, 9627–9632. [[CrossRef](#)]
35. Chng, E.L.K.; Sofer, Z.; Pumera, M. MoS<sub>2</sub> exhibits stronger toxicity with increased exfoliation. *Nanoscale* **2014**, *6*, 14412–14418. [[CrossRef](#)] [[PubMed](#)]
36. Pardo, M.; Shuster-Meiseles, T.; Levin-Zaidman, S.; Rudich, A.; Rudich, Y. Low cytotoxicity of inorganic nanotubes and fullerene-like nanostructures in human bronchial epithelial cells: Relation to inflammatory gene induction and antioxidant response. *Environ. Sci. Technol.* **2014**, *48*, 3457–3466. [[CrossRef](#)] [[PubMed](#)]
37. Appel, J.H.; Li, D.O.; Podlevsky, J.D.; Debnath, A.; Green, A.A.; Wang, Q.H.; Chae, J. Low Cytotoxicity and Genotoxicity of Two-Dimensional MoS<sub>2</sub> and WS<sub>2</sub>. *ACS Biomater. Sci. Eng.* **2016**, *2*, 361–367. [[CrossRef](#)]
38. Liu, S.; Shen, Z.; Wu, B.; Yu, Y.; Hou, H.; Zhang, X.X.; Ren, H.Q. Cytotoxicity and Efflux Pump Inhibition Induced by Molybdenum Disulfide and Boron Nitride Nanomaterials with Sheetlike Structure. *Environ. Sci. Technol.* **2017**, *51*, 10834–10842. [[CrossRef](#)]
39. Shang, E.; Niu, J.; Li, Y.; Zhou, Y.; Crittenden, J.C. Comparative toxicity of Cd, Mo, and W sulphide nanomaterials toward *E. coli* under UV irradiation. *Environ. Pollut.* **2017**, *224*, 606–614. [[CrossRef](#)]

40. Zou, W.; Zhang, X.; Zhao, M.; Zhou, Q.; Hu, X. Cellular proliferation and differentiation induced by single-layer molybdenum disulfide and mediation mechanisms of proteins via the Akt-mTOR-p70S6K signaling pathway. *Nanotoxicology* **2017**, *11*, 781–793. [[CrossRef](#)]
41. Zapór, L. Cytotoxicity Elicited by Molybdenum Disulphide in Different Size of Particles in Human Airway Cells. *Rocz. Ochr. Sr.* **2019**, *21*, 794–809.
42. Roy, D.; Das, A.K.; Saini, R.; Singh, P.K.; Kumar, P.; Hussain, M.; Mandal, A.; Dixit, A.R. Pulse current co-deposition of Ni-WS<sub>2</sub> nano-composite film for solid lubrication. *Mater. Manuf. Processes* **2017**, *32*, 365–372. [[CrossRef](#)]
43. Goldman, E.B.; Zak, A.; Tenne, R.; Kartvelishvili, E.; Levin-Zaidman, S.; Neumann, Y.; Stiubea-Cohen, R.; Palmon, A.; Hovav, A.-H.; Aframian, D.J. Biocompatibility of tungsten disulfide inorganic nanotubes and fullerene-like nanoparticles with salivary gland cells. *Tissue Eng. Part A* **2015**, *21*, 1013–1023. [[CrossRef](#)]
44. Garcia-Hevia, L.; Roehrer, I.; Mazzocchi, T.; Mencias, A.; Ricotti, L. Cytotoxicity of pristine and functionalized tungsten disulfide particles in the urinary system. *J. Nanopart. Res.* **2020**, *22*, 273. [[CrossRef](#)]
45. Domi, B.; Bhorkar, K.; Rumbo, C.; Sygellou, L.; Martin, S.M.; Quesada, R.; Yannopoulos, S.N.; Tamayo-Ramos, J.A. Toxicological assessment of commercial monolayer tungsten disulfide nanomaterials aqueous suspensions using human A549 cells and the model fungus *Saccharomyces cerevisiae*. *Chemosphere* **2021**, *272*, 129603. [[CrossRef](#)]
46. Pakdel, A.; Bando, Y.; Golberg, D. Nano boron nitride flatland. *Chem. Soc. Rev.* **2014**, *43*, 934–959. [[CrossRef](#)]
47. Horváth, L.; Magrez, A.; Golberg, D.; Zhi, C.; Bando, Y.; Smajda, R.; Horváth, E.; Forró, L.; Schwaller, B. In vitro investigation of the cellular toxicity of boron nitride nanotubes. *ACS Nano* **2011**, *5*, 3800–3810. [[CrossRef](#)]
48. Del Turco, S.; Ciofani, G.; Cappello, V.; Gemmi, M.; Cervelli, T.; Saponaro, C.; Nitti, S.; Mazzolai, B.; Basta, G.; Mattoli, V. Cytocompatibility evaluation of glycol-chitosan coated boron nitride nanotubes in human endothelial cells. *Colloids Surf. B Biointerfaces* **2013**, *111*, 142–149. [[CrossRef](#)]
49. Ciofani, G.; Raffa, V.; Mencias, A.; Cuschieri, A. Cytocompatibility, interactions, and uptake of polyethyleneimine-coated boron nitride nanotubes by living cells: Confirmation of their potential for biomedical applications. *Biotechnol. Bioeng.* **2008**, *101*, 850–858. [[CrossRef](#)]
50. Ciofani, G.; del Turco, S.; Rocca, A.; de Vito, G.; Cappello, V.; Yamaguchi, M.; Li, X.; Mazzolai, B.; Basta, G.; Gemmi, M.; et al. Cytocompatibility evaluation of gum Arabic-coated ultra-pure boron nitride nanotubes on human cells. *Nanomedicine* **2014**, *9*, 773–788. [[CrossRef](#)]
51. Xin, X.; Barger, M.; Roach, K.A.; Bowers, L.; Stefaniak, A.B.; Kodali, V.; Glassford, E.; Dunn, K.H.L.; Dunn, K.H.L.; Wolfarth, M.; et al. Toxicity evaluation following pulmonary exposure to an as-manufactured dispersed boron nitride nanotube (BNNT) material in vivo. *NanoImpact* **2020**, *19*, 100235. [[CrossRef](#)]
52. Campatelli, G.; Lorenzini, L.; Scippa, A. Optimization of process parameters using a Response Surface Method for minimizing power consumption in the milling of carbon steel. *J. Clean. Prod.* **2014**, *66*, 309–316. [[CrossRef](#)]
53. Rasel, M.A.I.; Li, T.; Nguyen, T.D.; Gu, Y.T. The assessment of toxicity of boron nitride nanoparticle using atomic forced microscopy. *IFMBE Proc.* **2015**, *52*, 31–34. [[CrossRef](#)]
54. Kodali, V.K.; Roberts, J.R.; Shoeb, M.; Wolfarth, M.G.; Bishop, L.; Eye, T.; Barger, M.; Roach, K.A.; Friend, S.; Schwegler-Berry, D.; et al. Acute in vitro and in vivo toxicity of a commercial grade boron nitride nanotube mixture. *Nanotoxicology* **2017**, *11*, 1040–1058. [[CrossRef](#)]
55. Wang, N.; Wang, H.; Tang, C.; Lei, S.; Shen, W.; Wang, C.; Wang, G.; Wang, Z.; Wang, L. Toxicity evaluation of boron nitride nanospheres and water-soluble boron nitride in *Caenorhabditis elegans*. *Int. J. Nanomed.* **2017**, *12*, 5941–5957. [[CrossRef](#)]
56. Kivanç, M.; Barutca, B.; Koparal, A.T.; Göncü, Y.; Bostancı, S.H.; Ay, N. Effects of hexagonal boron nitride nanoparticles on antimicrobial and antibiofilm activities, cell viability. *Mater. Sci. Eng. C* **2018**, *91*, 115–124. [[CrossRef](#)]
57. Kar, F.; Hacıoğlu, C.; Göncü, Y.; Söğüt, İ.; Şentürk, H.; Dönmez, D.B.; Kanbak, G.; Ay, N. In Vivo Assessment of the Effect of Hexagonal Boron Nitride Nanoparticles on Biochemical, Histopathological, Oxidant and Antioxidant Status. *J. Clust. Sci.* **2021**, *32*, 517–529. [[CrossRef](#)]
58. Sliwinska, A.; Kwiatkowski, D.; Czarny, P.; Milczarek, J.; Toma, M.; Korycinska, A.; Szymraj, J.; Sliwinski, T. Genotoxicity and cytotoxicity of ZnO and Al<sub>2</sub>O<sub>3</sub> nanoparticles. *Toxicol. Mech. Methods* **2015**, *25*, 176–183. [[CrossRef](#)]
59. Zhang, X.Q.; Yin, L.H.; Tang, M.; Pu, Y.P. ZnO, TiO<sub>2</sub>, SiO<sub>2</sub>, and Al<sub>2</sub>O<sub>3</sub> nanoparticles-induced toxic effects on human fetal lung fibroblasts. *Biomed. Environ. Sci.* **2011**, *24*, 661–669. [[CrossRef](#)]
60. Lin, W.; Stayton, I.; Huang, Y.W.; Zhou, X.D.; Ma, Y. Cytotoxicity and cell membrane depolarization induced by aluminum oxide nanoparticles in human lung epithelial cells A549. *Toxicol. Environ. Chem.* **2008**, *90*, 983–996. [[CrossRef](#)]
61. Nogueira, D.J.; Arl, M.; Köerich, J.S.; Simioni, C.; Ouriques, L.C.; Vicentini, D.S.; Matias, W.G. Comparison of cytotoxicity of  $\alpha$ -Al<sub>2</sub>O<sub>3</sub> and  $\eta$ -Al<sub>2</sub>O<sub>3</sub> nanoparticles toward neuronal and bronchial cells. *Toxicol. Vitro.* **2019**, *61*, 104596. [[CrossRef](#)]
62. Jeng, H.A.; Swanson, J. Toxicity of metal oxide nanoparticles in mammalian cells. *J. Environ. Sci. Health Part A* **2006**, *41*, 2699–2711. [[CrossRef](#)]
63. Zhu, X.; Zhu, L.; Duan, Z.; Qi, R.; Li, Y.; Lang, Y. Comparative toxicity of several metal oxide nanoparticle aqueous suspensions to Zebrafish (*Danio rerio*) early developmental stage. *J. Environ. Sci. Health Part A* **2008**, *43*, 278–284. [[CrossRef](#)]
64. Chen, L.; Yokel, R.A.; Hennig, B.; Toborek, M. Manufactured aluminum oxide nanoparticles decrease expression of tight junction proteins in brain vasculature. *J. Neuroimmune Pharmacol.* **2008**, *3*, 286–295. [[CrossRef](#)]

65. Oesterling, E.; Chopra, N.; Gavalas, V.; Arzuaga, X.; Lim, E.J.; Sultana, R.; Butterfield, D.A.; Bachas, L.; Hennig, B. Alumina nanoparticles induce expression of endothelial cell adhesion molecules. *Toxicol. Lett.* **2008**, *178*, 160–166. [[CrossRef](#)]
66. Sadiq, I.M.; Pakrashi, S.; Chandrasekaran, N.; Mukherjee, A. Studies on toxicity of aluminum oxide (Al<sub>2</sub>O<sub>3</sub>) nanoparticles to microalgae species: *Scenedesmus* sp. and *Chlorella* sp. *J. Nanopart. Res.* **2011**, *13*, 3287–3299. [[CrossRef](#)]
67. Ates, M.; Demir, V.; Arslan, Z.; Daniels, J.; Farah, I.O.; Bogatu, C. Evaluation of alpha and gamma aluminum oxide nanoparticle accumulation, toxicity, and depuration in *Artemia salina* larvae. *Environ. Toxicol.* **2015**, *30*, 109–118. [[CrossRef](#)]
68. Shirazi, A.; Shariati, F.; Keshavarz, A.K.; Ramezani, Z. Toxic Effect of Aluminum Oxide Nanoparticles on Green Micro-Algae *dunaliella salina*. *Int. J. Environ. Res.* **2015**, *9*, 585–594.
69. Srikanth, K.; Mahajan, A.; Pereira, E.; Duarte, A.C.; Rao, J.V. Aluminium oxide nanoparticles induced morphological changes, cytotoxicity and oxidative stress in Chinook salmon (CHSE-214) cells. *J. Appl. Toxicol.* **2015**, *35*, 1133–1140. [[CrossRef](#)]
70. Park, E.J.; Sim, J.; Kim, Y.; Han, B.S.; Yoon, C.; Lee, S.; Cho, M.H.; Lee, B.S.; Kim, J.H. A 13-week repeated-dose oral toxicity and bioaccumulation of aluminum oxide nanoparticles in mice. *Arch. Toxicol.* **2015**, *89*, 371–379. [[CrossRef](#)]
71. Rajiv, S.; Jerobin, J.; Saranya, V.; Nainawat, M.; Sharma, A.; Makwana, P.; Gayathri, C.; Bharath, L.; Singh, M.; Kumar, M.; et al. Comparative cytotoxicity and genotoxicity of cobalt (II, III) oxide, iron (III) oxide, silicon dioxide, and aluminum oxide nanoparticles on human lymphocytes in vitro. *Hum. Exp. Toxicol.* **2016**, *35*, 170–183. [[CrossRef](#)]
72. Benavides, M.; Fernández-Lodeiro, J.; Coelho, P.; Lodeiro, C.; Diniz, M.S. Single and combined effects of aluminum (Al<sub>2</sub>O<sub>3</sub>) and zinc (ZnO) oxide nanoparticles in a freshwater fish, *Carassius auratus*. *Environ. Sci. Pollut. Res.* **2016**, *23*, 24578–24591. [[CrossRef](#)]
73. Murali, M.; Suganthi, P.; Athif, P.; Bukhari, A.S.; Mohamed, H.S.; Basu, H.; Singhal, R. Histological alterations in the hepatic tissues of Al<sub>2</sub>O<sub>3</sub> nanoparticles exposed freshwater fish *Oreochromis mossambicus*. *J. Trace Elem. Med. Biol.* **2017**, *44*, 125–131. [[CrossRef](#)]
74. Akbaba, G.B.; Türkez, H. Investigation of the Genotoxicity of Aluminum Oxide,  $\beta$ -Tricalcium Phosphate, and Zinc Oxide Nanoparticles In Vitro. *Int. J. Toxicol.* **2018**, *37*, 216–222. [[CrossRef](#)] [[PubMed](#)]
75. Kim, Y.S.; Chung, Y.H.; Seo, D.S.; Choi, H.S.; Lim, C.H. Twenty-eight-day repeated inhalation toxicity study of aluminum oxide nanoparticles in male Sprague-Dawley rats. *Toxicol. Res.* **2018**, *34*, 343–354. [[CrossRef](#)]
76. Yousef, M.I.; Mutar, T.F.; Kamel, M.A.E.N. Hepato-renal toxicity of oral sub-chronic exposure to aluminum oxide and/or zinc oxide nanoparticles in rats. *Toxicol. Rep.* **2019**, *6*, 336–346. [[CrossRef](#)] [[PubMed](#)]
77. Yousef, M.I.; Al-Hamadani, M.Y.I.; Kamel, M.A. Reproductive Toxicity of Aluminum Oxide Nanoparticles and Zinc Oxide Nanoparticles in Male Rats. *Nano Part.* **2019**, *1*, 1–10. [[CrossRef](#)]
78. Anand, A.S.; Gahlot, U.; Prasad, D.N.; Kohli, E. Aluminum oxide nanoparticles mediated toxicity, loss of appendages in progeny of *Drosophila melanogaster* on chronic exposure. *Nanotoxicology* **2019**, *13*, 977–989. [[CrossRef](#)]
79. Boran, H.; Şaffak, S. Transcriptome alterations and genotoxic influences in zebrafish larvae after exposure to dissolved aluminum and aluminum oxide nanoparticles. *Toxicol. Mech. Methods* **2020**, *30*, 546–554. [[CrossRef](#)]
80. Lin, W.; Xu, Y.; Huang, C.-C.; Ma, Y.; Shannon, K.B.; Chen, D.-R.; Huang, Y.-W. Toxicity of nano- and micro-sized ZnO particles in human lung epithelial cells. *J. Nanopart. Res.* **2009**, *11*, 25–39. [[CrossRef](#)]
81. Brunner, T.J.; Wick, P.; Manser, P.; Spohn, P.; Grass, R.N.; Limbach, L.K. In vitro cytotoxicity of oxide nanoparticles: Comparison to asbestos, silica, and the effect of particle solubility. *Environ. Sci. Technol.* **2006**, *40*, 4374–4381. [[CrossRef](#)]
82. Aruoja, V.; Dubourguier, H.C.; Kasemets, K.; Kahru, A. Toxicity of nanoparticles of CuO, ZnO and TiO<sub>2</sub> to microalgae *Pseudokirchneriella subcapitata*. *Sci. Total Environ.* **2009**, *407*, 1461–1468. [[CrossRef](#)]
83. Kasemets, K.; Ivask, A.; Dubourguier, H.C.; Kahru, A. Toxicity of nanoparticles of ZnO, CuO and TiO<sub>2</sub> to yeast *Saccharomyces cerevisiae*. *Toxicol. Vitro.* **2009**, *23*, 1116–1122. [[CrossRef](#)]
84. Guan, R.; Kang, T.; Lu, F.; Zhang, Z.; Shen, H.; Liu, M. Cytotoxicity, oxidative stress, and genotoxicity in human hepatocyte and embryonic kidney cells exposed to ZnO nanoparticles. *Nanoscale Res. Lett.* **2012**, *7*, 602. [[CrossRef](#)] [[PubMed](#)]
85. Pasupuleti, S.; Alapati, S.; Ganapathy, S.; Anumolu, G.; Pully, N.R.; Prakhya, B.M. Toxicity of zinc oxide nanoparticles through oral route. *Toxicol. Ind. Health* **2012**, *28*, 675–686. [[CrossRef](#)] [[PubMed](#)]
86. Park, H.-S.; Kim, S.-J.; Lee, T.-J.; Kim, G.-Y.; Meang, E.; Hong, J.-S.; Kim, Y.-H.; Koh, S.-B.; Hong, S.-G.; Sun, Y.-S.; et al. A 90-day study of sub-chronic oral toxicity of 20nm positively charged zinc oxide nanoparticles in Sprague Dawley rats. *Intern. J. Nanomed.* **2014**, *9*, 93–107.
87. Davoren, M.; Herzog, E.; Casey, A.; Cottineau, B.; Chambers, D.; Byrne, H.J.; Lyng, F.M. In vitro toxicity evaluation of single walled carbon nanotubes on human A549 lung cells. *Toxicol. Vitro.* **2007**, *21*, 438–448. [[CrossRef](#)] [[PubMed](#)]
88. Zhang, L.W.; Zeng, L.; Barron, A.R.; Monteiro-Riviere, N.A. Biological interactions of functionalized single-wall carbon nanotubes in human epidermal keratinocytes. *Int. J. Toxicol.* **2007**, *26*, 103–113. [[CrossRef](#)]
89. Poland, C.A.; Duffin, R.; Kinloch, I.; Maynard, A.; Wallace, W.A.; Seaton, A.; Stone, V.; Brown, S.; MacNee, W.; Donaldson, K. Carbon nanotubes introduced into the abdominal cavity of mice show asbestos-like pathogenicity in a pilot study. *Nat. Nanotechnol.* **2008**, *3*, 423–428. [[CrossRef](#)]
90. Clichici, S.; Biris, A.R.; Catoi, C.; Filip, A.; Tabaran, F. Short-term splenic impact of single-strand DNA functionalized multi-walled carbon nanotubes intraperitoneally injected in rats. *J. Appl. Toxicol.* **2014**, *34*, 332–344. [[CrossRef](#)]
91. Reddy, A.R.N.; Krishna, D.R.; Himabindu, V.; Reddy, Y.N. Single walled carbon nanotubes induce cytotoxicity and oxidative stress in HEK293 cells. *Toxicol. Environ. Chem.* **2014**, *96*, 931–940. [[CrossRef](#)]

92. Dal Bosco, L.; Weber, G.E.; Parfitt, G.M.; Paese, K.; Gonçalves, C.O.; Serodre, T.M.; Furtado, C.A.; Santos, A.P.; Monserrat, J.M.; Barros, D.M. PEGylated carbon nanotubes impair retrieval of contextual fear memory and alter oxidative stress parameters in the rat hippocampus. *BioMed Res. Int.* **2015**, *2015*, 104135. [[CrossRef](#)]
93. Shang, S.; Yang, S.Y.; Liu, Z.M.; Yang, X. Oxidative damage in the kidney and brain of mice induced by different nano-materials. *Front. Biol.* **2015**, *10*, 91–96. [[CrossRef](#)]
94. Hosseinpour, M.; Azimirad, V.; Alimohammadi, M.; Shahabi, P.; Sadighi, M.; Nejad, G.G. The cardiac effects of carbon nanotubes in rat. *BioImpacts* **2016**, *6*, 79–84. [[CrossRef](#)] [[PubMed](#)]
95. Stoddart, M.J. *Cell Viability Assays: Introduction*; Humana Press: Totowa, NJ, USA, 2011. [[CrossRef](#)]
96. Nouzil, I.; Pervaiz, S.; Kannan, S. Role of jet radius and jet location in cryogenic machining of Inconel 718: A finite element method based approach. *Int. J. Interact. Des. Manuf.* **2021**, *15*, 1–19. [[CrossRef](#)]